Strain Energy on the Surface of an Anisotropic Half-Space Substrate: Effect of Quantum-Dot Shape and Depth

E. Pan[1,2], Y. Zhang[2], P. W. Chung[3] and M. Denda[4]

Abstract: Quantum-dot (QD) semiconductor synthesis is one of the most actively investigated fields in strain energy band engineering. The induced strain fields influence ordering and alignment, and the subsequent surface formations determine the energy bandgap of the device. The effect of the strains on the surface formations is computationally expensive to simulate, thus analytical solutions to the QD-induced strain fields are very appealing and useful. In this paper we present an analytical method for calculating the QD-induced elastic field in anisotropic half-space semiconductor substrates. The QD is assumed to be of any polyhedral shape, and its surface is approximated efficiently by a number of flat triangles. The problem is formulated as an Eshelby inclusion problem in continuum mechanics whose solution can be expressed by a volume-integral equation involving the Green's functions and the equivalent body-force of eigenstrain. By virtue of the point-force Green's function solution, this volume integral is subsequently reduced to a line integral over $[0, \pi]$ which is numerically integrated by the Gaussian quadrature.

Numerical examples are presented for cubic, pyramidal, truncated pyramidal and point QDs in GaAs (001) and (111) half-space substrates. The strain energy distribution on the surface of the substrate indicates clearly the strong influence of the QD shape and depth on the induced strain energy. This long-range strain energy on the surface has been found to be the main source for deter-

mining QD surface size and pattern.

Keyword: Quantum dot, misfit lattice, Green's function, GaAs semiconductor, strain energy

1 Introduction

Novel superlattice-based semiconductor devices have attracted considerable attention in recent years [Bimberg, Grundmann, and Ledentsov (1998); Stangl, Holy, and Bauer (2004); Jalabert, Coraux, Renevier, and Daudin (2005); Ferdous and Haque (2007)] where semiconductor quantum dots (QDs), nanowires and nanorods have been intensively investigated [Leonard, Krishnamurthy, Reaves, Denbaars, and Petroff (1993); Gosling and Willis (1995); Baxter and Aydil (2005)]. Self-assembled quantum dots have been of particular interest because of their three-dimensional (3D) confinement of charge carriers and excitons, and hence their potential in nano-scale electronic devices [Petroff (2003); Friedman (2007); Levine, Golovin, and Davis (2007)].

It is well known that the elastic fields produced by QDs substantially influence surface feature formations that consequently affect the electronic band structure. As either a detector or emitter of electromagnetic signals, the bandgap energy determines the operational wavelength in say, the photovoltaic mode, of the semiconductor element. Hence, the elastic fields induced by QDs have to be studied in order to obtain a well ordered QD structure. To analyze the elastic fields in and around the QDs and other quantum structures, several methods have been proposed, such as the finite element and finite difference methods [Grundmann, Stier, and Bimberg (1995); Benabbas (1996); Matagne, Leburton, Destine, and Cantraine (2000); Liu and Quek (2002); Pei, Lu,

[1] Corresponding author. Email: pan2@uakron.edu

[2] Dept. of Civil Engineering and Dept. of Applied Mathematics, University of Akron, Akron, OH 44325

[3] U.S. Army Research Laboratory, Aberdeen Proving Ground, MD 21005

[4] Dept. of Mechanical and Aerospace Engineering, Rutgers University, Piscataway, NJ 08854

and Wang (2003); Jonsdottir, Halldorsson, Beltz, and Romanov (2006)], atomistic modeling [Pryor, Kim, Wang, Williamson, and Zunger (1998); Califano and Harrison (2000); Kikuchi, Sugii, and Shintani (2001); Makeev and Madhukar (2001)], and analytical approaches [Jogai (2000); Glas (2001); Pan and Jiang (2004); Zhang and Sharma (2005)]. In particular, the Green's function solutions have been proposed and applied to QD studies [Pan and Yang (2001)]. Because of their accuracy and efficiency, the analytical methods, particularly the Green's function method, are arguably more appealing to experimentalists and physical device designers in the studies of QD structures [Andreev, Downes, Faux, and O'Reilly (1999); Pearson and Faux (2000)]. There are also other multiscale approaches which can be employed to the QD modeling [e.g., Ghoniem and Cho (2002); Ma, Liu, Lu, and Komanduri (2006); Ma, Lu, Wang, Hornung, Wissink, and Komanduri (2006); Orsini, Power, and Morvan (2008)]. More recently, the multiscale Green's functions have been also introduced to model QD- or other defects-induced strain field [Tewary (2004); Tewary and Read (2004); Yang and Tewary (2005); Yang and Tewary (2006); Read and Tewary (2007)], which have been shown to be computationally efficient. However, while the lattice Green's functions have been well-developed so far, the corresponding continuum Green's functions still require further study, particularly when considering semiconductor anisotropy.

In this paper, we present an analytical method for the QD-induced strain field in half-space semiconductor substrates under the assumption of continuum elasticity. We point out that, under the epitaxial growth, the misfit strain within the QD could be gradient, instead of uniform distribution [Malachia, Kycia, Medeiros-Ribeiro, Magalhaes-Paniago, Kamins, and Williams (2003)], and as such, the material property in the QD could be difficult to calibrate [Zhu, Pan, Chung, Cai, Liew and Buldum (2006)]. Thus, the simplified well-known inclusion model will be adopted in this paper. It was verified recently that the inclusion model could predict slightly different results as compared to the inhomogeneity model using

the bulk property of the QD (about 10% within the strained quantum structures, see, e.g., [Yang and Pan (2002); Pan, Han, and Albrecht (2005)]). Under these assumptions, we derive our solution based on the Green's function method in terms of the Stroh formalism with the corresponding exact integration of the Green's functions over the QD surface (composed of piece-wise flat triangles). This paper is organized as follows: In section 2, the strained QD system is described. In section 3, the surface of the QD is approximated by a number of flat triangles over which the area integration is carried out exactly so that the induced elastic fields can be expressed in terms of a simple line integral over $[0, \pi]$. If the QD is a point source, then the QD-induced elastic fields can be analytically expressed by the point-force Green's functions in the half-space. In section 4, numerical examples are carried out for buried cubic, pyramidal, truncated pyramidal, and point QDs in the GaAs half-space substrate with different growth orientations. The effects of the QD shape and depth on the strain energy are discussed. Conclusions are drawn in section 5.

2   Problem Description and Boundary Integral Expressions of the Misfit-strain Induced Elastic Field in Anisotropic Semiconductors

We assume that the QD and its substrate are both linear elastic. Therefore, the governing equations for the QD semiconductor system can be described by

$$\sigma_{ij,i} + f_j = 0 \qquad (1)$$

$$\sigma_{ij} = C_{ijkl}\gamma_{kl} \qquad (2)$$

$$\gamma_{ij} = \frac{1}{2}(u_{i,j} + u_{j,i}) \qquad (3)$$

where u_i, σ_{ij} and γ_{ij} are the displacement, stress and strain, respectively, C_{ijlm} the elastic stiffness tensor, and f_j the body force.

The lattice mismatch between the dot and the substrate manifests itself through a misfit strain γ_{ij}^* inside the QD. The constitutive equation (2) is therefore modified as

$$\sigma_{ij} = C_{ijkl}(\gamma_{kl} - \gamma_{kl}^*) \qquad (4)$$

Substitution of (4) into the equilibrium equation (1) leads to

$$C_{ijkl}u_{k,li} = C_{ijkl}\gamma^*_{kl,i} \qquad (5)$$

The right-hand side of Eq. (5), defined as

$$f_j = -C_{ijkl}\gamma^*_{kl,i} \qquad (6)$$

is the equivalent body force of the misfit-strain or eigenstrain γ^*_{ij} within the QD domain.

We now assume that the 3D point-force Green's functions are given for the half-space substrate, then for the general eigenstrain γ^*_{ij} at $\mathbf{x} = (x_1, x_2, x_3)$ within the QD domain V, the induced displacement at $\mathbf{d} = (d_1, d_2, d_3)$ can be found using the method of superposition. That is, the response is an integral, over V, of the equivalent body force defined by (6), multiplied by the point-force Green's functions, as

$$u_k(\mathbf{d}) = -\int_V U^k_j(\mathbf{x};\mathbf{d})[C_{ijlm}\gamma^*_{lm}(\mathbf{x})]_{,i}dV(\mathbf{x}) \qquad (7)$$

where $U^k_j(\mathbf{x};\mathbf{d})$ is the j-th Green's elastic displacement at $\mathbf{x}$ due to a point force in the k-th direction applied at $\mathbf{d}$.

Integrating by parts and noting that the eigenstrain is nonzero only in the QD domain V, Eq. (7) can be expressed alternatively as

$$u_k(\mathbf{d}) = \int_V U^k_{j,x_i}(\mathbf{x};\mathbf{d})C_{ijlm}\gamma^*_{lm}(\mathbf{x})dV(\mathbf{x}) \qquad (8)$$

If we further assume that the eigenstrain is constant within the QD domain V, then the domain integration can be transformed to the boundary integration. That is

$$u_k(\mathbf{d}) = C_{ijlm}\gamma^*_{lm}\int_{\partial V} U^k_j(\mathbf{x};\mathbf{d})n_i(\mathbf{x})dS(\mathbf{x}) \qquad (9)$$

where $n_i(\mathbf{x})$ is the outward normal on the boundary ∂V of the QD.

In order to find the elastic strain, we take the derivatives of Eq. (9) with respect to the observation point $\mathbf{d}$ (i.e., the source point of the point-force Green's function), which yields $(k, p=1,2,3)$

$$\gamma_{kp}(\mathbf{d}) = \frac{1}{2}\gamma^*_{lm}C_{ijlm}\int_{\partial V}\left[U^k_{j,d_p}(\mathbf{x};\mathbf{d}) + U^p_{j,d_k}(\mathbf{x};\mathbf{d})\right]$$

$$n_i(\mathbf{x})dS(\mathbf{x}) \qquad (10)$$

The stresses inside the QD are obtained from Eq. (4), and outside from Eq. (2).

It is obvious that in order to solve the QD-induced elastic field, the key is to carry out the surface integration involved in (9) and (10). This requires the integral of the corresponding half-space Green's functions, which is discussed below.

3 Analytical Integration of the Half-space Green's Function over a Flat Triangle

We assume that the boundary of the QD can be approximated by a number of flat triangles. We want to analytically integrate the half-space Green's functions over one of the flat triangles. To do so, we first briefly review the half-space Green's functions in general anisotropic semiconductors.

The half-space point-force Green's function with source point at $\mathbf{d}$ and field point at $\mathbf{x}$ can be expressed as a sum of an explicit infinite-space solution and a complementary part in terms of a line integral over $[0, \pi]$ [Pan (2002)]

$$\mathbf{U}(\mathbf{x};\mathbf{d}) = \mathbf{U}^\infty(\mathbf{x};\mathbf{d}) + \frac{1}{2\pi^2}\int_0^\pi \overline{\mathbf{A}}\mathbf{G}_1\mathbf{A}^T d\theta \qquad (11)$$

where the overbar means complex conjugate, superscript T denotes matrix transpose, and

$$(\mathbf{G}_1)_{ij} =$$

$$\frac{(\overline{\mathbf{B}}^{-1}\mathbf{B})_{ij}}{-\overline{p}_i x_3 + p_j d_3 - [(x_1-d_1)\cos\theta + (x_2-d_2)\sin\theta]} \qquad (12)$$

We point out that, on the right-hand side of Eq. (11), the first term corresponds to the Green's displacement tensor in an anisotropic infinite space. Its integration over a flat triangle was presented by Wang *et al.* [Wang, Denda, and Pan (2006)]. Also in Eqs. (11) and (12), the Stroh eigenvalues p_j, and eigenmatrices $\mathbf{A}$ and $\mathbf{B}$ are all functions of θ, as well as the elastic stiffness tensor of the semiconductor materials.

In order to find the misfit strain-induced elastic fields, we also need the derivatives of the Green's displacement tensor with respect to the field point (x_1, x_2, x_3) of the Green's function [Pan (1999)].

They are found to be (j=1, 2, 3)

$$\frac{\partial U(x;d)}{\partial x_j} = \frac{\partial U^\infty(x;d)}{\partial x_j} - \frac{1}{2\pi^2}\int_0^\pi \overline{A}G_2 \langle g_j \rangle A^T d\theta$$

(13)

where

$$(G_2)_{ij} =$$

$$\frac{(\overline{B}^{-1}B)_{ij}}{\{-\overline{p}_i x_3 + p_j d_3 - [(x_1-d_1)\cos\theta + (x_2-d_2)\sin\theta]\}^2}$$

(14)

$$\langle g_1 \rangle = diag[\cos\theta, \cos\theta, \cos\theta]$$
$$\langle g_2 \rangle = diag[\sin\theta, \sin\theta, \sin\theta] \qquad (15)$$
$$\langle g_3 \rangle = diag[\overline{p}_1, \overline{p}_2, \overline{p}_3]$$

Again, since the integration on a flat triangle has already been presented for the infinite part of the half-space Green's function [Wang, Denda, and Pan (2006)], we only need to present the integration of the complementary part of the Green's function, i.e., the integration of the second term on the right-hand side of Eq. (13).

We consider first the integration of the Green's displacement tensor. Again, we assume that the QD surface can be effectively approximated by a number of flat triangles. Therefore, the integral expression of Eq. (9) over a flat triangle, Δ, is

$$u_k(d) = C_{ijlm}\gamma^*_{lm}n_i \int_\Delta U_j^k(x;d)dA(x) \qquad (16)$$

where n_i is the outward normal to the flat triangle Δ. Substituting Eq. (11) into (16) and changing the integration orders, the contribution from the complementary part can be expressed as

$$u_k(d) = \frac{1}{2\pi^2}C_{ijlm}\gamma^*_{lm}n_i \int_0^\pi \overline{A}\left[\int_\Delta G_1 d\Delta(x)\right]A^T d\theta$$

(17)

While the outside line integration can be easily carried out by employing Gaussian quadrature, we discuss the area integration over the flat triangle, which can be done analytically as will be shown below. Actually, since in the expression

for G_1 in Eq. (12), its numerator is a function of θ only, the integration over the flat triangle Δ needs to be carried out for the following expression only

$$F_1(d_j, \theta) =$$

$$\int_\Delta \frac{d\Delta(x)}{-\overline{p}_i x_3 + p_j d_3 - [(x_1-d_1)\cos\theta + (x_2-d_2)\sin\theta]}$$

(18)

Similarly, in order to find the QD-induced strain field, (Eqs. (10) and (13)), one needs only to carry out the following area integration over the flat triangle.

$$F_2(d_j, \theta) =$$

$$\int_\Delta \frac{d\Delta(x)}{\{-\overline{p}_i x_3 + p_j d_3 - [(x_1-d_1)\cos\theta + (x_2-d_2)\sin\theta]\}^2}$$

(19)

We now carry out the area integration over a flat triangle in Eqs. (18) and (19) exactly. To do so, we introduce the following transformation between the global coordinate system x (x_1, x_2, x_3) and local coordinate system ξ (ξ_1, ξ_2, ξ_3) associated with the flat triangle (Fig. 1)

$$\begin{bmatrix} x_1 - x_{01} \\ x_2 - x_{02} \\ x_3 - x_{03} \end{bmatrix} = \begin{bmatrix} a_{11} & a_{12} & a_{13} \\ a_{21} & a_{22} & a_{23} \\ a_{31} & a_{32} & a_{33} \end{bmatrix} \begin{bmatrix} \xi_1 \\ \xi_2 \\ \xi_3 \end{bmatrix} \qquad (20)$$

Then, the integration becomes (n=1,2)

$$F_n(d_j, \theta) = \int_0^h d\xi_2 \int_{-l_1+l_1\xi_2/h}^{l_2-l_2\xi_2/h} d\xi_1$$

$$\frac{1}{[f_1(d_j,\theta)\xi_1 + f_2(d_j,\theta)\xi_2 + f_3(d_j,\theta)]^n} \qquad (21)$$

where

$$f_1(d_j, \theta) = -(\overline{p}_i a_{31} + a_{11}\cos\theta + a_{21}\sin\theta) \quad (22)$$

$$f_2(d_j, \theta) = -(\overline{p}_i a_{32} + a_{12}\cos\theta + a_{22}\sin\theta) \quad (23)$$

$$f_3(d_j, \theta) = -\overline{p}_i(x_{03} + a_{33}\xi_3) + p_j d_3 + d_1\cos\theta$$
$$+ d_2\sin\theta - (x_{01} + a_{13}\xi_3)\cos\theta$$
$$- (x_{02} + a_{23}\xi_3)\sin\theta \qquad (24)$$

Table 1: Maximum strain energy E_{max} on the surface of the substrate GaAs (with orientations (001) and (111)) for different QD shapes with different depths (unit of energy=118.8×10^{15}Nm).

Depth	Orientation/Location		Cubic	Truncated pyramid	Pyramid
d=1nm	(001)	E_{max}	2.54	2.93	2.71
		(x, y)	$(\pm1, \pm1)$	$(\pm1, \pm1)$	$(0,0)$
	(111)	E_{max}	2.55	2.75	2.05
		(x, y)	$(1,0)$	$(1,0)$	$(0,0)$
d=2nm	(001)	E_{max}	1.77	1.99	0.96
		(x, y)	$(0,0)$	$(0,0)$	$(0,0)$
	(111)	E_{max}	1.31	1.34	0.75
		(x, y)	$(0,0)$	$(0,0)$	$(0,0)$
d=3nm	(001)	E_{max}	1.03	1.09	0.41
		(x, y)	$(0,0)$	$(0,0)$	$(0,0)$
	(111)	E_{max}	0.70	0.70	0.36
		(x, y)	$(0,0)$	$(0,0)$	$(0,0)$

The integration can now be carried out, and the results are

$$F_1(d_j, \theta) = \frac{1}{f_1} \left[\frac{f_1 l_2 + f_3}{f_2 - f_1 l_2/h} \ln \left(\frac{f_2 h + f_3}{f_1 l_2 + f_3} \right) \right.$$
$$\left. - \frac{-f_1 l_1 + f_3}{f_2 + f_1 l_1/h} \ln \left(\frac{f_2 h + f_3}{-f_1 l_1 + f_3} \right) \right] \quad (25)$$

$$F_2(d_j, \theta) = \frac{1}{f_1} \left[\frac{1}{f_2 + f_1 l_1/h} \ln \left(\frac{f_2 h + f_3}{-f_1 l_1 + f_3} \right) \right.$$
$$\left. - \frac{1}{f_2 - f_1 l_2/h} \ln \left(\frac{f_2 h + f_3}{f_1 l_2 + f_3} \right) \right] \quad (26)$$

With these exact expressions, the QD-induced displacement and strain fields can be finally expressed in terms of the line integration over [0, π] (e.g., Eq. (17) for the induced displacements). Again, the line integration can be carried out numerically using 8-point Gaussian quadrature.

4 Numerical Examples

We now apply our analytical solutions to calculate the strain energy induced by a buried QD within the GaAs half-space substrate. The surface of the substrate is traction free. The QD is located at a depth d below the surface (Fig. 2) and the misfit strain is hydrostatic, i.e., $\gamma_{xx}^* = \gamma_{yy}^* = \gamma_{zz}^* = 0.07$. We point out that this misfit strain is relatively large and the corresponding nonlinear influence will be pursued in the future using other methods,

such as the multiscale meshless method [Shen and Atluri (2004)]. As for the QD shape, we assume it to be either cubic, pyramidal, truncated pyramidal, or point type. The QDs have the same height h (=4nm, except for the point QD). To make all the QDs (including the point QD) the same volume, we have the base length 2.155h for cubic QD, upper length 1.79h and lower length 2.5h for truncated pyramid QD, base length 3.732h for pyramid QD (Fig.2). The point QD is located at the middle height of the cubic QD (i.e., its vertical distance to the surface is $d + h/2$). We study the effect of the QD shape and depth on the strain energy on the surface.

Shown in Figs. 3(a)-(d) are, respectively, contours of the normalized strain energy on the surface of GaAs (001) (top row) and GaAs (111) (bottom row), induced by a buried cubic, truncated pyramidal, pyramidal and point QD. In this example, the depth d=2nm, height h=4nm, and the strain energy is normalized by 118.8×10^{15}Nm (this normalization factor is also used below for the strain energy) (Table 1). It is clear that different QD shapes (including point QD) induce different strain energy distributions on the surface of the substrate. Besides the difference on the contour shape, the strain energy values are also different. For example, the contours with values 0.3, 0.6 and 0.9 (corresponding, respectively, to the heavy blue, red and black curves) move towards the center when the QD shape changes
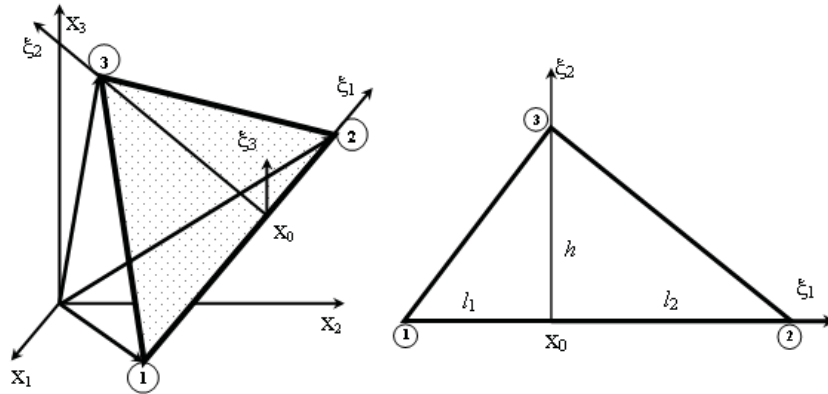
Figure 1: Geometry of the flat triangle D (with corners 1,2,3), and transformation from the global (x_1, x_2, x_3) to local (ξ_1, ξ_2, ξ_3) coordinates where ξ_3 is along the outward normal direction of the flat triangle.
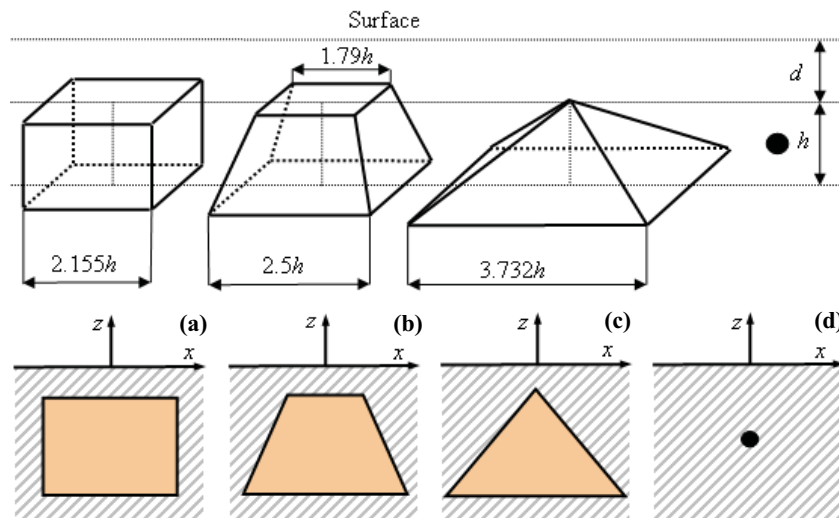

Figure 2: Geometry for (a) a cubic QD, (b) a truncated pyramid QD, (c) a pyramid QD, and (d) a point QD. Top row is the 3D view and bottom row is the vertical x-z plan view. All these QDs have the same volume.
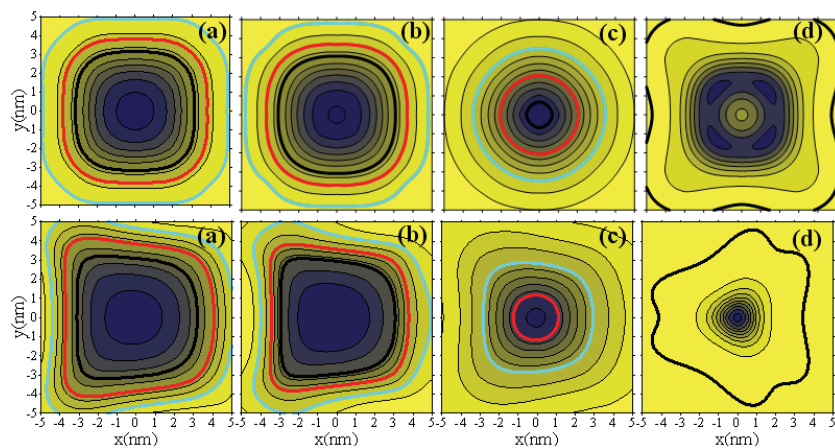

Figure 3: Normalized strain energy on the surface of the half-space substrate of GaAs (001) (top row) and GaAs (111) (bottom row) induced by (a) a cubic, (b) a truncated pyramid, (c) a pyramid, and (d) a point QD, where the heavy blue, red and black lines correspond to the normalized strain energy values of 0.3, 0.6 and 0.9 respectively. The QD is embedded within the substrate with its top side at depth d=2nm from the surface.
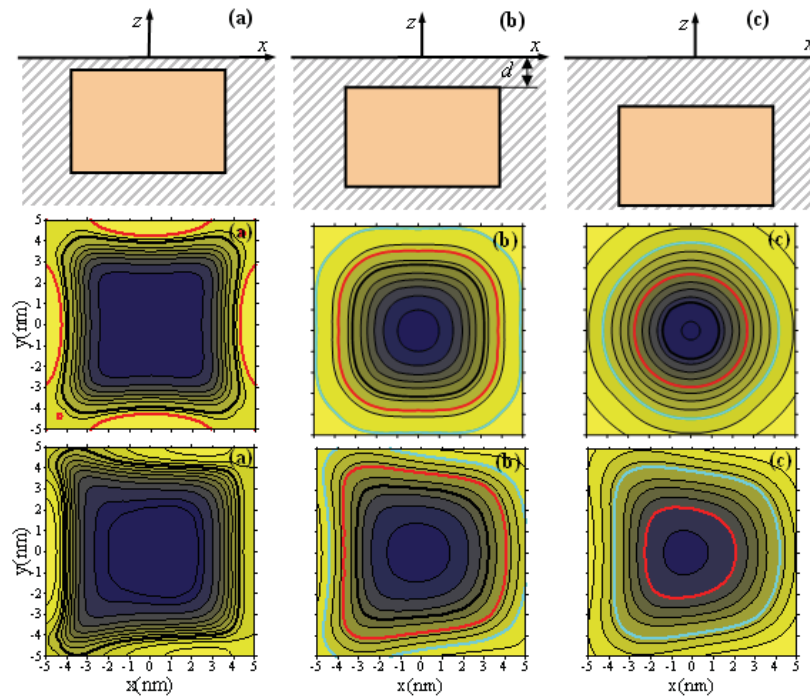
Figure 4: Geometry of a cubic QD within a half-space substrate with different depth *d*: the vertical x-z plan view (top row), and the strain energy induced by the cubic QD in substrate GaAs (001) (middle row) and GaAs (111) (bottom row): (a) *d*=1, (b) *d*=2, and (c) *d*=3. The heavy blue, red and black lines correspond to the normalized strain energy values of 0.3, 0.6 and 0.9, respectively.
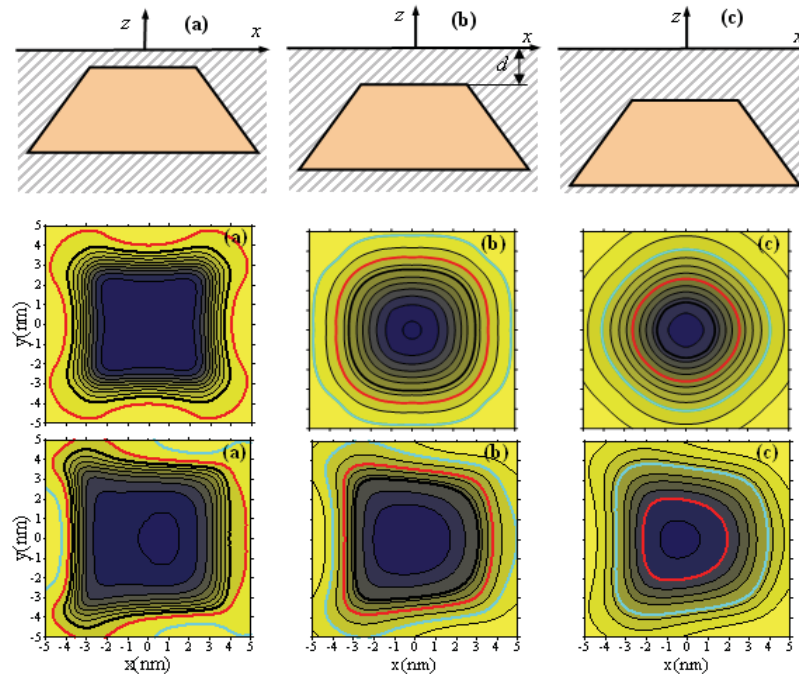

Figure 5: Geometry of a truncated pyramid QD within a half-space substrate with different depth *d*: the vertical x-z plan view (top row), and the strain energy induced by the truncated pyramid QD in substrate GaAs (001) (middle row) and GaAs (111) (bottom row): (a) *d*=1, (b) *d*=2, and (c) *d*=3. The heavy blue, red and black lines correspond to the normalized strain energy values of 0.3, 0.6 and 0.9, respectively.

Figure 6: Geometry of a pyramid QD within a half-space substrate with different depth d: the vertical x-z plan view (top row), and the strain energy induced by the pyramid QD in substrate GaAs (001) (middle row) and GaAs (111) (bottom row): (a) $d=1$, (b) $d=2$, and (c) $d=3$. The heavy blue, red and black lines correspond to the normalized strain energy values of 0.3, 0.6 and 0.9, respectively.
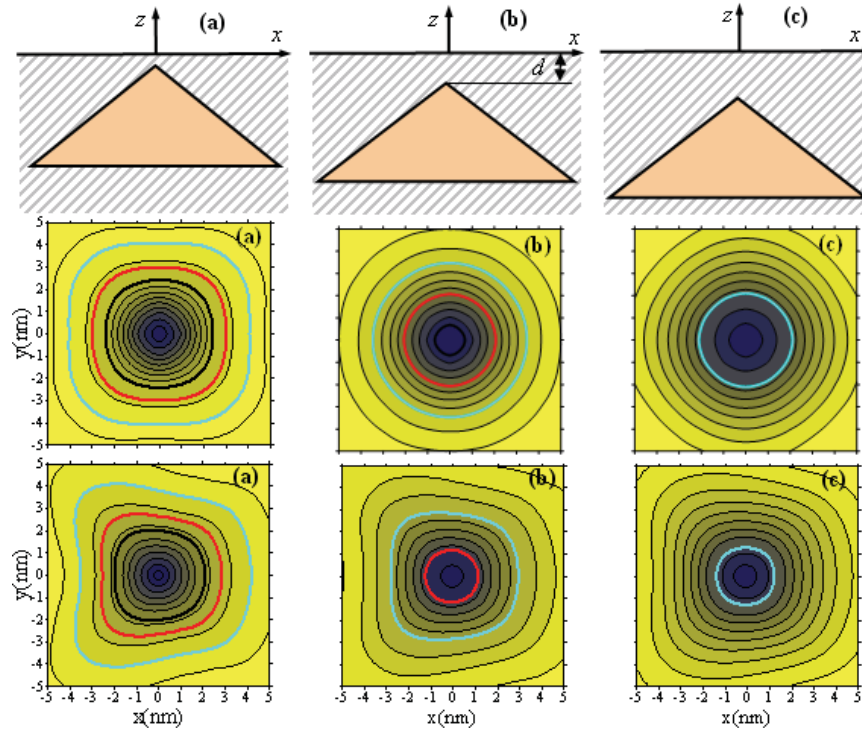
from left to right (i.e., cubic, truncated pyramid, and pyramid, except for the point QD which has a much large strain energy magnitude as compared to other finite-size QDs). Table 1 lists the maximum strain energy values corresponding to different QD shapes at different depths within the GaAs substrate with both (001) and (111) orientations. It is clear, from Table 1, that while the induced maximum strain energy value decreases with increasing depth, its value on the substrate GaAs (001) is always larger than that on the corresponding inclined substrate GaAs (111). Furthermore, the effect of the QD shapes (cubic, truncated pyramid, pyramid, and point QD) on the strain energy is complicated, as can be seen from Figs. 3(a)-(d). Also from Figs. 3(a)-(d), it is observed, by comparing the top row to the bottom row, that the contour shapes of the strain energy over GaAs (001) are sharply different to those over GaAs (111).

We now study the effect of QD depth on the strain energy distribution on the surface where the maxi-

mum strain energy values for different QD depths are listed in Table 1. The top row of Fig. 4 shows the depths of the cubic QD within the substrate with $d=1$nm, 2nm, and 3nm, whilst the strain energy distributions on the surface of GaAs (001) and (111) are shown, respectively, in the middle and bottom rows. Again, the heavy blue, red and black contour lines correspond, respectively, to the strain energy values of 0.3, 0.6, and 0.9. It is apparent from Fig. 4 that as the QD moves away from the surface, the strain energy contour shape approaches to those due to a point QD with equal volume.

Similar numerical results are shown in Figs. 5 and 6, respectively, for the truncated pyramidal and pyramidal QDs. While the strain energy distributions induced by the pyramidal QD are similar to those by an equivalent-volume QD, those by cubic and truncated pyramidal QD are different. These again demonstrate the effect of the QD shape and depth on the misfit-lattice induced strain energy in

the QD system.

5 Conclusions

In this paper, we presented an analytical method for calculating the QD-induced strain energy fields in half-space semiconductor substrates. The QD is assumed to be of any polyhedral shape which can be efficiently approximated by a number of flat triangles. We studied cubic, pyramidal, truncated pyramidal and point QDs within the GaAs (001) and GaAs (111) half-space substrates. Numerical results illustrate that the shape of the QDs has apparent influence on the strain energy distribution on the surface, so is the depth of the QDs. These results should be interesting to the overgrowth of QDs on the substrate where the long-range strain energy on the surface plays an important role in controlling the new QD shapes and patterns.

References

Andreev, A. D.; Downes, J. R.; Faux, D. A.; O'Reilly, E. P. (1999): Strain distributions in quantum dots of arbitrary shape. *J. Appl. Phys.*, vol. 86, pp. 297-305.

Baxter, J. B.; Aydil, E. S. (2005): Epitaxial growth of Zn0 Nanowires on a- and c-plane sapphire. *J. Cryst. Growth*, vol. 274, pp. 407-411.

Benabbas, T.; Francois, P.; Androussi, Y.; Lefebvre A. (1996): Stress relaxation in highly strained InAs/GaAs structures as studied by finite element analysis and transmission electron microscopy. *J. Appl. Phys.*, vol. 80, pp. 2763-2767.

Bimberg, D.; Grundmann, M.; Ledentsov, N. N. (1998): Quantum dot heterostructures. *Wiley, New York*.

Califano, M.; Harrison P. (2000): Presentation and experimental validation of a single-band, constant-potential model for self-assembled InAs/GaAs quantum dots. *Phys. Rev. B*, vol. 61, pp. 10959-10965.

Ferdous, F.; Haque, A. (2007): Effect of elastic strain redistribution on electronic band structures of compressively strained GalnAsP/Inp membrane quantum wires. *J. Appl. Phys.*, vol. 101, pp. 093106-5.

Friedman, L. H. (2007): Anisotropy and order of epitaxial self-assembled quantum dots. *Phy. Rev. B*, vol. 75, pp. 193302-4.

Ghoniem, N. M.; Cho, K. (2002): The emerging role of multiscale modeling in nano- and micromechanics of materials. *CMES: Computer Modeling in Engineering and Sciences,* vol.3, pp. 147-174.

Glas, F. (2001): Elastic relaxation of truncated pyramidal quantum dots and quantum wires in a half space: An analytical calculation. *J. Appl. Phys.*, vol. 90, pp. 3232-3241.

Gosling, T. J.; Willis, J. R. (1995): Mechanical stability and electronic-properties of buried strained quantum-wire arrays. *J. Appl. Phys.*, vol. 77, pp. 05601-05610.

Grundmann, M.; Stier, O.; Bimberg, D. (1995): InAs/GaAs pyramidal quantum dots: Strain distribution, optical phonons, and electronic structure. *Phy. Rev. B*, vol. 52, pp. 11969-11981.

Jalabert, D.; Coraux, J.; Renevier, H.; Daudin, B. (2005): Deformation profile in GaN quantum dots: Medium-energy ion scattering experiments and theoretical calculations. *Phy. Rev. B*, vol. 72, pp. 115301-5.

Jogai, B. (2000): Three-dimensional strain field calculations in coupled InAs/GaAs quantum dots. *J. Appl. Phys.*, vol. 88, pp. 5050-5055.

Jonsdottir, F.; Halldorsson D.; Beltz G. E.; Romanov A. E. (2006): Elastic fields and energies of coherent surface islands. *Modelling Simul. Mater. Sci. Eng.*, vol. 14, pp. 1167-1180.

Kikuchi, Y.; Sugii, H.; Shintani, K. (2001): Strain profiles in pyramidal quantum dots by means of atomistic simulation. *J .Appl. Phys.*, vol. 89, pp. 1191-1196.

Leonard, D.; Krishnamurthy, M.; Reaves, C. M.; Denbaars, S.P.; Petroff, P. M. (1993): Direct formation of quantum-sized dots from uniform coherent islands of InGaAs on GaAs surfaces. *Appl. Phys. Lett.*, vol. 63, pp. 3203-3205.

Levine, M. S.; Golovin, A. A.; Davis, S. H. (2007): Self-assembly of quantum dots in a thin epitalxial film wetting and elastic substrate. *Phy. Rev. B*, vol. 75, pp. 205312-11.

Liu, G. R.; Quek Jerry S. S. (2002): A finite element study of the stress and strain fields of InAs quantum dots embedded in GaAs. *Semicond. Sci. Technol.*, vol. 17, pp. 630-643.

Ma, J.; Liu, Y.; Lu, H.; Komanduri, R. (2006): Multiscale simulation of nanoindentation using the generalized interpolation material point (GIMP) method, dislocation dynamics (DD) and molecular dynamics (MD). *CMES: Computer Modeling in Engineering & Sciences,* vol.16, pp. 41-56.

Ma, J.; Lu, H.; Wang, B.; Hornung, R.; Wissink, A.; Komanduri, R. (2006): Multiscale simulation of using generalized interpolation material point (GIMP) method and molecular dynamics (MD). *CMES: Computer Modeling in Engineering & Sciences,* vol.14, pp. 101-118.

Makeev, M. A.; Madhukar, A. (2001): Simulations of atomic level stresses in systems of buried Ge /Si islands. *Phys. Rev. Lett.*, vol. 86, pp. 5542-5545.

Malachia, A.; Kycia, S.; Medeiros-Ribeiro, G.; Magalhaes-Paniago, R.; Kamins, T. I.; Williams, R. S. (2003): 3D Composition of Epitaxial Nanocrystals by Anomalous X-ray Diffractions: Observation of a Si-Rich Core in Ge Domes on Si(100). *Physical Review Letters*, vol. 91, pp. 176101-4.

Matagne, P.; Leburton, J. P.; Destine, J.; Cantraine, G. (2000): Modeling of the Electronic Properties of Vertical Quantum Dots by the Finite Element Method. *CMES: Computer Modeling in Engineering & Sciences*, vol. 1, pp. 1-10.

Orsini, P.; Power, H.; Morvan, H. (2008): Improving volume element methods by meshless radial basis function techniques. *CMES: Computer Modeling in Engineering & Sciences,* vol.23, pp.

187-208.

Pan, E. (1999): A BEM analysis of fracture mechanics in 2D anisotropic piezoelectric solids. *Eng. Anal. Bound. Elements*, vol. 23, pp. 67-76.

Pan, E. (2002): Mindlin's problem for an anisotropic piezoelectric half-space with general boundary conditions. *Proc. R. Soc. Lond. A*, vol. 458, pp. 181-208.

Pan, E.; Jiang, X. (2004): Effect of QWR Shape on the Induced Elastic and Piezoelectric Fields. *CMES: Computer Modeling in Engineering & Sciences,* vol.6, pp. 77-90.

Pan, E.; Yang, B. (2001): Elastostatic fields in an anisotropic substrate due to a buried quantum dot. *J. Appl. Phys.*, vol. 90, pp. 6190-6196.

Pan, E.; Han, F.; Albrecht, J. D. (2005): Strain Fields in InAs/GaAs Quantum Wire Structures: Inclusion vs. Inhomogeneity. *Journal of Applied Physics*, vol. 98, pp. 013534-12.

Pearson, G. S.; Faux, D. A. (2000): Analytical solutions for strain in pyramidal quantum dots. *J. Appl. Phys.*, vol. 88, pp. 730-736.

Pei, Q. X.; Lu, C.; Wang, Y. Y. (2003): Effect of elastic anisotropy on the elastic fields and vertical alignment of quantum dots. *J. Appl. Phy.*, vol. 93, pp. 1487-1492.

Petroff, P. M. (2003): Epitaxial growth and electronic structure of self-assembled quantum dots. *Top. Appl. Phys.*, vol. 90, pp. 1-25.

Pryor, C.; Kim, J.; Wang, L. W.; Williamson, A. J.; Zunger, A. (1998): Comparison of two methods for describing the strain profiles in quantum dots. *J. Appl. Phys.*, vol. 83, pp. 2548-2554.

Read, D. T.; Tewary, V. K. (2007): Multiscale model of near-spherical germanium quantum dots in silicon. *Nanotechnology*, vol. 18, pp.105402-12.

Shen, S. P.; Atluri, S. N. (2004): Multiscale Simulation Based on the Meshless Local Petrov-Galerkin (MLPG) Method. *CMES: Computer Modeling in Engineering & Sciences*, vol. 5, pp. 235-255.

Stangl, J.; Holy, V.; Bauer, G. (2004): Structural properties of self-organized semiconductor nanostructures. *Rev. Mod. Phys.*, vol. 76**,** pp.725-

783.

Tewary, V. K. (2004): Multiscale Green's-function method for modeling point defects and extended defects in anisotropic solids: Application to a vacancy and free surface in copper. *Phys. Rev. B*, vol. 69, pp. 094109-13.

Tewary, V. K.; Read, D. T. (2004): Integrated Green's Function Molecular Dynamics Method for Multiscale Modeling of Nanostructures: Application to Au Nanoisland in Cu. *CMES: Computer Modeling in Engineering & Sciences*, vol. 6, pp. 359-372.

Wang, C. Y.; Denda, M.; Pan, E. (2006): Analysis of quantum-dot-induced strain and electric fields in piezoelectric semiconductors of general anisotropy. *International Journal of Solids and Structures*, vol. 43, pp. 7593-7608.

Yang, B.; Pan, E. (2002): Elastic Analysis of an Inhomogeneous Quantum Dot in Multilayered Semiconductors Using a Boundary Element Method. *Journal of Applied Physics*, vol. 92, pp. 3084-3088.

Yang, B.; Tewary, V. K. (2005): Green's function-based multiscale modeling of defects in a semi-infinite silicon substrate. *International Journal of Solids and Structures*, vol. 42, pp. 4722-4737.

Yang, B.; Tewary, V. K. (2006): Efficient Green's function modeling of line and surface defects in multilayered anisotropic elastic and piezoelectric materials. *CMES: Computer Modeling in Engineering & Sciences*, vol. 15, pp. 165-178.

Zhang, X.; Sharma, P. (2005): Size Dependency of Strain in Arbitrary Shaped, Anisotropic Embedded Quantum Dots due to Nonlocal Dispersive Effects. *Physical Review B*, vol. 72, pp. 195345-16.

Zhu, R.; Pan, E.; Chung, P. W.; Cai, X.; Liew, K. M.; Buldum, A. (2006): Atomistic Calculation of Elastic Moduli in Strained Silicon. *Semiconductor Science and Technology*, vol. 21, pp. 906-911.